NUMERICAL SIMULATION OF THE GENERALIZED MAXWELL–STEFAN MODEL FOR MULTICOMPONENT DIFFUSION IN MICROPOROUS SORBENTS*

Jan-Baptist W. P. Loos, Peter J. T. Verheijen and Jacob A. Moulijn

Department of Chemical Process Technology, Delft University of Technology, Julianalaan 136, 2628 BL Delft, The Netherlands

Received September 13, 1991
Accepted October 22, 1991

The results of simulations of transient multicomponent surface diffusion in a microporous adsorbent are given for various conditions. The generalized Maxwell–Stefan theory was applied to describe the diffusion phenomena. The diffusion equations were solved numerically. The transient uptake of a binary mixture and the counterdiffusion of two sorbate species in a slab were simulated. Some striking phenomena of multicomponent diffusion are presented. The relation to the approximate solution obtained by the linearized theory of multicomponent mass transfer is discussed. The simulations are compared with various results found in the literature.

Separation and conversion processes taking place on solid sorbents, e.g. zeolites often proceed under non-equilibrium conditions. The understanding and modelling of the diffusion behaviour of mixtures in these materials has practical importance because of its influence on the selectivity of these separations and reactions. Surface diffusion is also of fundamental interest in physical chemistry. In principle, a molecule moving over a surface can be seen as a probe of the interactions with the surface and with the other molecules in its vicinity.

Diffusion in micropores (size smaller than 2 nm) is strongly temperature and concentration dependent. The diffusing molecules never really leave the force field of the surface. In zeolites the intracrystalline pores or openings are of molecular dimensions and the diffusing molecules are likely to hinder each other at high surface occupancies. Multicomponent diffusion behaviour is of special interest. The transient uptake of a mixture of a fast diffusing-weakly adsorbing species and a slow diffusing--strongly adsorbing species in zeolites is typical: the uptake of the fast diffusing species exceeds the equilibrium value in the approach to the equilibrium situation (see e.g. refs[1–4]).

The transient uptake of mixture components in microporous sorbents has been

* Presented as a poster at the *International Symposium "Zeolite Chemistry and Catalysis", Prague, September 8–13, 1991.*

simulated numerically by Round et al.[5] (using a simplified Onsager approach, neglecting cross terms). Marutovsky and Bülow[4,6] described multicomponent diffusion in zeolites by the generalized Fick approach and the linear driving force model. Krishna[7] applied the generalized Maxwell–Stefan (GMS) approach to surface or temperature activated diffusion. The linearized theory of multicomponent mass transfer[8,9] was used to obtain solutions of the last two models mentioned.

Here, the objective is to numerically simulate the transient uptake of mixtures in microporous adsorbent particles, with the most rigorous model possible, thereby avoiding the earlier used approximations.

THEORETICAL

The transient diffusion behaviour of a binary mixture in an infinite plane slab is simulated. The equation of continuity or conservation of mass connects concentration and diffusive flux in the adsorbent:

$$n_s \nabla_t \theta_i(z, t) + \nabla_z J_i(z, t) = 0 \quad (i = 1, 2 \ldots n) . \tag{1}$$

We may combine this equation with an equation describing the phenomenon of the diffusive surface flux to obtain the diffusion equation. To this end the generalized Maxwell–Stefan equations were applied. This results in a set of nonlinear coupled partial differential equations (PDE). With the proper initial and boundary conditions this is sufficient to determine uniquely the functions $\theta_i(z, t)$.

Generalized Maxwell–Stefan Theory

The generalized Maxwell–Stefan equations[7]

$$-\frac{\theta_i}{RT} \nabla(\mu_i)_{T,\phi} = \sum_{j=1}^{n+1} \frac{\theta_i \theta_j}{\mathscr{D}_{ij}} (u_i - u_j) = \sum_{j=1}^{n+1} \frac{\theta_j J_i - \theta_i J_j}{n_s \mathscr{D}_{ij}} \quad (i = 1, 2, \ldots n) \tag{2}$$

employ the gradients of the chemical potentials as driving forces, in agreement with the theory of irreversible thermodynamics. The influence of the substrate is incorporated in the model by considering the vacant sites V to be the $(n + 1)$th constituent of the system[7]. It is pseudo-species to which thermodynamic quantities can be assigned. Only n GMS-equations are independent because the Gibbs–Duhem equation gives an extra relation. Surface diffusion is a special case. There can be no drift velocity of the $(n + 1)$ component mixture. Since the total number of sites is fixed, the vacancy flux balances the fluxes of adsorbed species. For sorption of two species the physical interpretation of Eq. (2) is as follows[10]. The driving force of component 1 is balanced by the frictional drag on molecules 1 moving past those of component 2 with a relative velocity $(u_1 - u_2)$, weight factor $\theta_1\theta_2$ and inter-

molecular drag coefficient $1/\mathscr{D}_{12}$ and of molecules 1 moving past the surface sites (component V) with a relative velocity $(u_1 - u_V)$, weight factor $\theta_1\theta_V$ and drag coefficient $1/\mathscr{D}_{1V}$. The Onsager reciprocal relations show that the GMS diffusivities are symmetrical:

$$\mathscr{D}_{ij} = \mathscr{D}_{ji} \quad (i, j = 1, 2, \ldots n, V) . \tag{3}$$

The GMS diffusivities $\mathscr{D}_{iV}$ can be related to single sorbate diffusivities[7]. The GMS diffusivity $\mathscr{D}_{12}$, describing the interchange of species 1 and 2 adsorbed on the surface, is interpolated between two limiting values

$$\lim_{\theta_1 \to 1} \mathscr{D}_{12} = \mathscr{D}_{1V} , \quad \lim_{\theta_2 \to 1} \mathscr{D}_{12} = \mathscr{D}_{2V} , \tag{4}$$

by the multicomponent Vignes equation[7]

$$\mathscr{D}_{12} = (\mathscr{D}_{12})_{\theta_1 \to 1}^{\theta_1/(\theta_1+\theta_2)} \cdot (\mathscr{D}_{12})_{\theta_2 \to 1}^{\theta_2/(\theta_1+\theta_2)} = (\mathscr{D}_{1V})^{\theta_1/(\theta_1+\theta_2)} \cdot (\mathscr{D}_{2V})^{\theta_2/(\theta_1+\theta_2)} . \tag{5}$$

The gradient of the chemical potential can be expressed in the gradients of fractional coverages:

$$\frac{\theta_i}{RT} \nabla_z(\mu_i)_{T,\phi} = \theta_i \sum_{j=1}^{n} \frac{\partial \mu_i}{\partial \theta_j} \frac{d\theta_j}{dz} = \sum_{j=1}^{n} \Gamma_{ij} \frac{d\theta_j}{dz} \quad (i = 1, 2, \ldots n) . \tag{6}$$

The result is that thermodynamic factors Γ_{ij} are introduced in the equations. These factors increase with total occupancy in the case of convex isotherms. For a Langmuir type adsorption isotherm

$$\theta_i = \frac{b_i p_i}{1 + \sum_{j=1}^{n} b_j p_j} \quad (i = 1, 2, \ldots n) , \tag{7}$$

describing the equilibrium between an ideal binary gas mixture and a solid adsorbent, the factors are given in the Appendix (Eq. (*15*)).

The GMS-equations (*2*) in combination with Eq. (*6*) may be written[7] in n-dimensional matrix form to give explicit relations for the fluxes

$$(J) = -n_s[B]^{-1}[\Gamma] \frac{d(\theta)}{dz} , \tag{8}$$

where $[B]^{-1}$ contains the GMS diffusivities. Substitution of Eq. (*8*) in the continuity equations (*1*) leads to the diffusion equations. From this notation the relation with the generalized Fick approach[7] becomes apparent:

$$[D] = [B]^{-1}[\Gamma] . \tag{9}$$

In the Appendix the elements of $[B]^{-1}$ and $[D]$ are given. The GMS approach, starting from physically meaningful drag coefficients, results in a concentration dependence of the Fick diffusivities $[D]$, composed of transport and thermodynamic factors.

In general, different saturation capacities n_s will exist for different molecules. The surface occupancies may be expressed in the number of sites covered per unit area instead of the number of molecules adsorbed per unit area. The total number of sites may be defined by e.g. $n_{s,1}$, the saturation capacity of species 1. By this definition the number of sites is fixed and the vacancy flux balances the fluxes of sites covered by species 1 and 2. We only have to multiply the flux of sites covered by species 2 by $n_{s,2}/n_{s,1}$ to obtain the mole flux of species 2. The values of $\mathscr{D}_{ij}$ do not depend on the definition.

Numerical Solution Method

The differential equations describing the model are non-linear and must be solved numerically. The continuum equations were discretized in the x-coordinate by an explicit finite difference approximation[11]. This leads to a set of coupled first order differential equations for each slice. The discretized versions of the PDE's were integrated in time using a fourth-order Runge–Kutta procedure with variable stepsize. The procedure solves stiff equations by a semi-implicit method and non-stiff by an explicit method. The Runge–Kutta procedure estimates the stepsize within the maximum stepsize Δt allowed. The finite difference approximations for the fluxes are:

$$(J_1) = [D(\theta(\pm 1, t))] \frac{(\theta(\pm 1, t) - \theta_1)}{\Delta x/2},$$

$$(J_k) = \left[D\left(\frac{\theta_{k-1} + \theta_k}{2}\right)\right] \frac{(\theta_{k-1} - \theta_k)}{\Delta x} \quad (k = 2 \ldots N), \tag{10}$$

$$(J_{N+1}) = 0.$$

The initial conditions (IC) and the boundary conditions (BC) for transient uptake are

$$\theta_i(x, 0) = 0; \quad -1 < x < 1; \quad t = 0,$$

$$\theta_i(\pm 1, t) = \theta_{io}; \quad x = \pm 1; \quad t < 0, \tag{11}$$

$$\frac{\partial}{\partial x} \theta_i(0, t) = 0; \quad x = 0; \quad t \geqq 0.$$

A discontinuity exists at $(x, t) = (\pm 1, 0)$ in the concentration functions $\theta_i(x, t)$. Since $[D]$ depends on the concentrations (Eq. (16)) there is also a discontinuity

in $[D]$ at the start. An alternative scheme was also attempted to avoid the discontinuity in $[D]$:

$$(J_k) = [D(\theta_k)] \frac{(\theta_{k-1} - \theta_k)}{\Delta x} \quad (k = 1 \ldots N). \tag{12}$$

The local truncation errors introduced by these boundary layer effects do not penetrate the solution and decay provided the method is stable. The stability, the growth of the deviation from the true solution, cannot be derived for a non-linear problem. In that case the stability does not only depend on the finite difference scheme but also on the solution being obtained. If the solution becomes unbounded for bounded input values and oscillates with increasing amplitude it is termed unstable.

RESULTS AND DISCUSSION

Simulations were performed at boundary conditions near saturation. In this situation the molecules will hinder each other most and multicomponent effects are likely to be more pronounced.

Effect of Grid Size

The behaviour in the boundary layer is the main concern. The finite difference approximation is a poor one at the boundary where the gradients at the start will be infinitely large. Use of Eq. (*10*) leads to stable solutions depending on the input values. The local truncation errors decay and an accurate solution is obtained. This is shown in Fig. 1 (solid curves 2–4 coincide). The errors may oscillate with decaying amplitude when the discontinuities in (θ) and $[D]$ are large. Decreasing Δt and increasing Δx may eliminate the oscillations.

Use of another difference scheme, Eq. (*12*), does not lead to oscillations for these input values used, but the solution is inaccurate. Refining the grid prevents to a certain

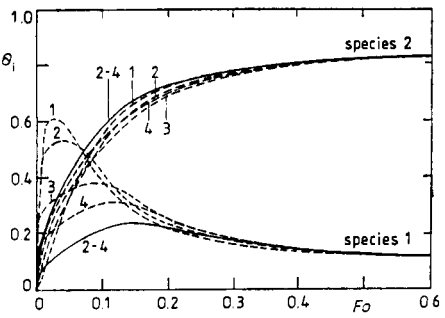

FIG. 1

Convergence of the numerical solutions. Eq. (*12*): broken lines, Eq. (*10*): solid lines. Curves: 1 $\Delta x = 0{\cdot}2$; 2 $\Delta x = 0{\cdot}10$; 3 $\Delta x = 0{\cdot}05$; 4 $\Delta x = 0{\cdot}025$, $\Delta Fo = 1 \cdot 10^{-5}$. IC: $\theta_1(x, 0) = \theta_2(x, 0) = 0$. BC: $\theta_1(\pm 1, t) = 0{\cdot}10$; $\theta_2(\pm 1, t) = 0{\cdot}85$, $\mathscr{D}_{1V}/\mathscr{D}_{2V} = 100$

extent the solution from being swamped by the boundary layer effects and this solution converges to the solution using Eq. (*10*) (Fig. 1).

All simulations in Figs 2–6 were carried out for $\Delta x = 0{\cdot}025$ and $\Delta Fo = 1 \cdot 10^{-5}$ using Eq. (*10*).

Round et al.[8] obtained solutions of a simplified Onsager model numerically. These model equations can also be solved by the numerical procedure used to solve the GMS model. The following equations for the fluxes were used:

$$J_i = -n_s L_{ii} \theta_i \frac{\nabla \mu_i}{RT} \quad (i = 1, 2 \ldots n) . \tag{13}$$

The Onsager coefficients L_{11} and L_{22} were assumed constant and the cross coefficients L_{12} and L_{21} were assumed zero. This means that the matrix $[B]^{-1}$ may be replaced in the numerical procedure by the diagonal matrix $[L]$. The results of Round et al.[8] were reproduced.

Effect of the Ratio of GMS *Diffusivities and the Boundary Conditions*

The transient uptake of a binary mixture of sorbate molecules was simulated for several diffusivity ratios $\mathscr{D}_{1V}/\mathscr{D}_{2V}$. This is shown in Figs 2 and 3 for different boundary conditions. In all cases a maximum in the uptake of the fastest diffusing species 1 is observed. The height of the maximum relative to the equilibrium value

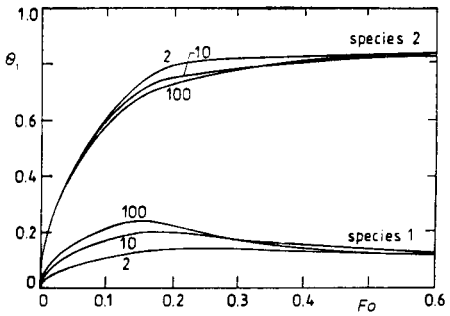

FIG. 2

Transient uptake of a binary mixture in a plane slab as function of the Fourier number for various ratios of diffusivities $\mathscr{D}_{1V}/\mathscr{D}_{2V}$, as indicated. IC: $\theta_1(x, 0) = \theta_2(x, 0) = 0$. BC: $\theta_1(\pm 1, t) = 0{\cdot}10$; $\theta_2(\pm 1, t) = 0{\cdot}85$

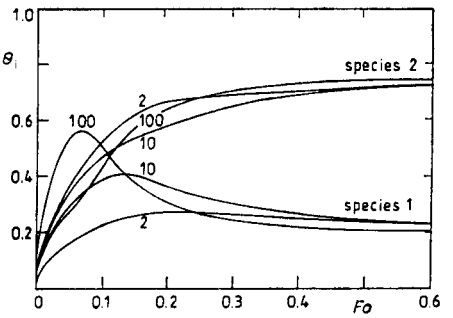

FIG. 3

Transient uptake of a binary mixture in a plane slab as function of the Fourier number for variours ratios of diffusivities $\mathscr{D}_{1V}/\mathscr{D}_{2V}$, as indicated. IC: $\theta_1(x, 0) = \theta_2(x, 0) = 0$, BC: $\theta_1(\pm 1, t) = 0{\cdot}20$; $\theta_2(\pm 1, t) = 0{\cdot}75$

is approximately the same in Figs 2 and 3. Decreasing $\mathscr{D}_{1V}$ results in a lower and broader maximum. The uptake of species 2 is not much affected by variation of $\mathscr{D}_{1V}$. The ratio of the uptake of both species is nearly constant up to the maximum in the curve. From then on molecules 1 are replaced by molecules 2 and the curves are symmetrical with respect to a horizontal line in Figs 2 and 3.

The counterdiffusion behaviour, the (partial) replacement of species 1 by species 2 and vice versa was also simulated. Both cases are shown in Fig. 4. The exchange of the slow diffusing component by the fast diffusing component is faster than the exchange of the fast diffusing component by a slow diffusing component. The numerical solution leads to the same result as the approximate solution by Krishna[7]. The uptake of species 1 and desorption of species 2 is accelerated because the decreasing frictional drag $(1/\mathscr{D}_{12})$ between these components with increasing concentration of species 1 (Eq. (5)) facilitates the interchange of molecules 1 and 2.

Concentration Profiles

The concentration profiles in a half-slab are shown in Fig. 5 for various Fourier numbers. The solutions are symmetrical with respect to the center of the slab. At the start both species diffuse in the direction of decreasing concentration. For $0{\cdot}01 < Fo < 0{\cdot}12$ species 1 diffuses against its gradient and the local concentration of

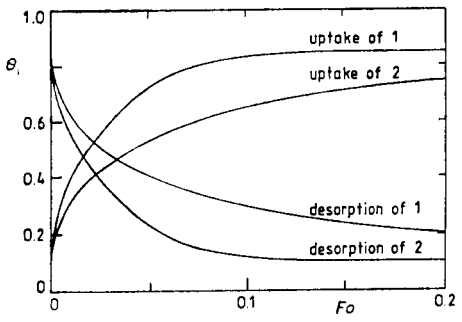

FIG. 4

Transient counterdiffusion of species 1 and 2 in a slab. $\mathscr{D}_{1V}/\mathscr{D}_{2V} = 100$. Replacement of species 2 by species 1, IC: $\theta_1(x, 0) = 0{\cdot}10$; $\theta_2(x, 0) = 0{\cdot}85$. BC: $\theta_1(\pm 1, t) = 0{\cdot}85$; $\theta_2(\pm 1, t) = 0{\cdot}10$. Replacement of species 1 by species 2, IC: $\theta_1(x, 0) = 0{\cdot}85$; $\theta_2(x, 0) = 0{\cdot}10$. BC: $\theta_1(\pm 1, t) = 0{\cdot}10$; $\theta_2(\pm 1, t) = 0{\cdot}85$

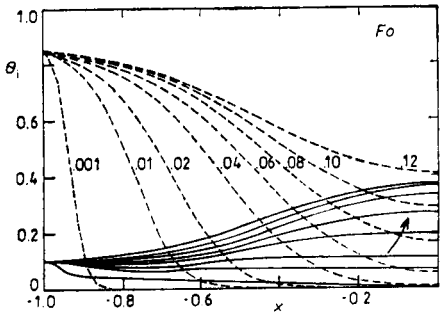

FIG. 5

Profiles of concentration vs distance for $\mathscr{D}_{1V}/\mathscr{D}_{2V} = 100$. IC: $\theta_1(x, 0) = \theta_2(x, 0) = 0$. BC: $\theta_1(\pm 1, t) = 0{\cdot}10$; $\theta_2(\pm 1, t) = 0{\cdot}85$. Solid line: species 1, broken line: species 2

this species exceeds the equilibrium concentration. This behaviour can be understood from the physical picture of the GMS-model. The gradient of the chemical potential of species 2, the thermodynamic force of component 2 acts on component 1 via the friction of molecules 2 on 1. Where the gradient of species 2 is large, this may lead to species 1 diffusing against its gradient. Beyond the maximum ($Fo > 0{\cdot}12$) the profiles have become symmetrical with respect to a horizontal line in Fig. 5 and counterdiffusion sets in.

Comparison with the Approximate Solution

The GMS model for transient uptake in microporous sorbents was solved by Krishna[7] using the linearized theory of multicomponent mass transfer[8,9]. This theory relies on the assumption of constancy of the Fick diffusivity matrix $[D]$ along the diffusion path. However, $[D]$ is a function of the concentrations and will have to be calculated at average concentrations when using this method. With this assumption, the uptake of n species is the n-dimensional matrix analog of the single sorbate uptake solution F. The square matrix function $[F]$ of the averaged Fickian matrix can be evaluated after a small time interval ΔFo using Sylvester's theorem (see e.g. ref.[7]). The new concentrations so obtained are used to calculate $[D]$ for the next time interval and so on. The procedure starts with the Fickian matrix calculated for an empty particle. The numerical procedure starts with very different values of $[D]$, especially when the boundary concentrations are high. The maximum calculated by the approximate method for the same conditions is much higher (Fig. 6). The better agreement with the solutions obtained by use of Eq. (*12*) (Fig. 1, curve 1) can be understood from the fact that this scheme also starts with $[D]$ calculated at zero concentrations. For smaller grid sizes this solution converges to the numerical solution obtained via Eq. (*10*). In general the approximation will be less accurate in the first part of the solution and when the discontinuities at the boundary are large.

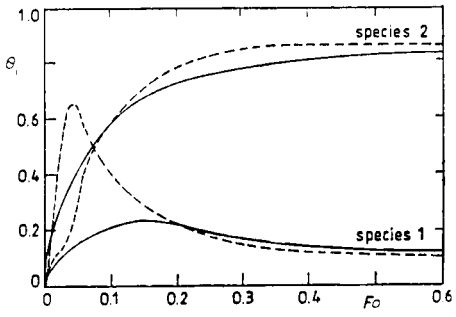

FIG. 6

Comparison with the approximate solution ($\Delta Fo = 0{\cdot}0018$) obtained by the linearized theory. IC: $\theta_1(x, 0) = \theta_2(x, 0) = 0$. BC: $\theta_1(\pm 1, t) = 0{\cdot}10$; $\theta_2(\pm 1, t) = 0{\cdot}85$. $\mathscr{D}_{1V}/\mathscr{D}_{2V} = 100$

Comparison with Experiment

The simulations in Figs 2 and 3 are very similar in shape to measurements of the transient uptake of nitrogen and methane in zeolite A by Habgood[1]. The loading of nitrogen overshoots its equilibrium value as in Fig. 2. For a higher boundary concentration of nitrogen it overshoots the loading of methane as well, as in Fig. 3. The same was observed[4] for the mixture uptake of benzene and heptane in zeolite X. The uptake of mixtures of carbon dioxide and sulfur dioxide in mordenite was studied by Ma and Roux[2]. These uptake curves are very similar in shape to the simulations in Fig. 2.

CONCLUSIONS

Solutions of the GMS model for surface diffusion were obtained by this numerical method. The solutions for transient uptake compare well with experimental transient uptake curves of binary mixtures in zeolites found in the literature. The simulated concentration profiles in a slab clarify the multicomponent diffusion effects found in zeolites.

To apply the Maxwell-Stefan approach in the description of transient multicomponent surface diffusion a numerical solution method is necessary. Application of the linearized theory may lead to a significant deviation. The reason for the different results is the strong dependence of the Fick diffusivities on the concentrations in a Langmuirian sorbed phase, especially when the total occupancy of the sites is high. This dependence is mainly due to the influence of the thermodynamic correction factors in the Fick diffusivities. Adsorption isotherms for microporous sorbents are usually strongly non-linear and near saturation this leads to a high sensitivity of these factors on concentration. The linearized theory relies on the assumption of constant Fick diffusivities along the diffusion path. In many cases of surface diffusion this assumption is not a good one at the start of the uptake and errors will occur in this region of the solution.

The authors would like to thank dr. ir. A. W. Gerritsen for providing the code of the Runge–Kutta procedure.

SYMBOLS

$[A]$	$= [B]^{-1}$ with elements A_{ij}
b_i	coefficient in Langmuir isotherm, Eq. (7), m^2/N
$[B]$	matrix of inverted GMS-diffusivities defined by Eq. (8), s/m^2
$\mathscr{D}_{ij}$	GMS diffusivity, m/s^2
$[D]$	matrix of Fick diffusivities with elements D_{ij}, m^2/s
F	single sorbate function giving the approach to equilibrium
Fo	$= \mathscr{D}_{2V}t/l^2$ Fourier number

(J) column vector of diffusive fluxes, mol/ms
$[L]$ matrix of Onsager coefficients with elements L_{ij}, m^2/s
l half-thickness of the slab, m
n number of sorbates
n_s total surface concentration at saturation, mol/m^2
N number of slices in the half-slab
p_i partial pressure of i in the bulk phase, N/m^2
R gas constant, J/mol/K
t time, s
T temperature, K
u velocity of diffusion, m/s
x $= z/l$ dimensionless distance from the center of the slab
z distance from the center of the slab, m
$[\Gamma]$ matrix of thermodynamic correction factors defined by Eq. (6) with elements Γ_{ij}
μ_i chemical potential of i, J/mol
ϕ spreading pressure, N/m
(θ) column vector of fractional surface occupancies

Subscripts

i, j, 1, 2 refers resp. to species i, j, 1, 2
k refers to the number of the slice in the slab
s refers to surface property
t refers to time
T, ϕ refers to gradient obtained under conditions of constant temperature and spreading pressure
V refers to vacancies
z refers to coordinate along diffusion path

Mathematical Symbols

[ ] square matrix of dimension n
( ) vector of dimension n

REFERENCES

1. Habgood H. W.: Can. J. Chem. *36*, 1384 (1958).
2. Ma Y. H., Roux A. J.: AIChE J. *19*, 1055 (1973).
3. Carlson N. W., Dranoff J. S. in: *Proc. 2nd Eng. Found. Conf. on Fund. of Adsorption 1987*, (A. I. Liapis, Ed.), p. 129.
4. Marutovsky R. M., Bülow M.: Z. Phys. Chem. (Lepizig) *263*, 849 (1982).
5. Round G. F., Habgood H. W., Newton R.: Sep. Sci. *1*, 219 (1966).
6. Marutovsky R. M., Bülow M.: Chem. Eng. Sci. *42*, 2745 (1987).
7. Krishna R.: Chem. Eng. Sci. *45*, 1779 (1990).
8. Toor H. L.: AIChE J. *10*, 448; *10*, 460 (1964).
9. Stewart W. E., Prober R.: Ind. Eng. Chem., Fundam. *3*, 224 (1964).
10. Krishna R., Taylor R. in: *Handbook of Heat and Mass Transfer Operations* (N. P. Cheremisinoff, Ed.), Vol. 2, Chap. 7. Gulf, 1986.
11. Ames F. A.: *Numerical Methods for Partial Differential Equations*, 2nd ed., Chap. 2. Academic Press, New York 1977.

APPENDIX[7]

The elements of $[A] = [B]^{-1}$ for diffusion of a mixture of two sorbates in a sorbent are:

$$A_{11} = \mathscr{D}_{1V}(\theta_1\mathscr{D}_{2V} + (1 - \theta_1)\,\mathscr{D}_{12})/(\theta_1\mathscr{D}_{2V} + \theta_2\mathscr{D}_{1V} + \theta_V\mathscr{D}_{12})$$

$$A_{12} = \theta_1\mathscr{D}_{2V}(\mathscr{D}_{1V} - \mathscr{D}_{12})/(\theta_1\mathscr{D}_{2V} + \theta_2\mathscr{D}_{1V} + \theta_V\mathscr{D}_{12})$$

$$A_{21} = \theta_2\mathscr{D}_{1V}(\mathscr{D}_{2V} - \mathscr{D}_{12})/(\theta_1\mathscr{D}_{2V} + \theta_2\mathscr{D}_{1V} + \theta_V\mathscr{D}_{12})$$

$$A_{22} = \mathscr{D}_{2V}(\theta_2\mathscr{D}_{1V} + (1 - \theta_2)\,\mathscr{D}_{12})/(\theta_1\mathscr{D}_{2V} + \theta_2\mathscr{D}_{1V} + \theta_V\mathscr{D}_{12})\,. \qquad (14)$$

The elements of the matrix of thermodynamic factors $[\Gamma]$ in the case of a binary Langmuir adsorption isotherm are:

$$\Gamma_{12} = \frac{\theta_1}{1 - \theta_1 - \theta_2}\,, \quad \Gamma_{11} = 1 + \Gamma_{12}\,,$$

$$\Gamma_{21} = \frac{\theta_2}{1 - \theta_1 - \theta_2}\,, \quad \Gamma_{22} = 1 + \Gamma_{21}\,. \qquad (15)$$

The element of the Fickian matrix $[D]$ are obtained by matrix multiplication (Eq. (9)):

$$D_{11} = A_{11}\Gamma_{11} + A_{12}\Gamma_{21}$$

$$D_{12} = A_{11}\Gamma_{12} + A_{12}\Gamma_{22}$$

$$D_{21} = A_{21}\Gamma_{11} + A_{22}\Gamma_{21}$$

$$D_{22} = A_{21}\Gamma_{12} + A_{22}\Gamma_{22}\,. \qquad (16)$$